

RESEARCH ARTICLE

## Investigation of the Antifungal Activity of Curcumin-Coated Gold Nanoparticles

Shahram Mahmoudi<sup>1</sup>, Seyed Mohammad Amini<sup>2\*</sup>, Sadegh Khodavaissy<sup>3</sup>, Kosar Mansoori<sup>4</sup>

<sup>1</sup> Department of Parasitology and Mycology, School of Medicine, Iran University of Medical Sciences, Tehran, Iran

<sup>2</sup> Microbial Biotechnology Research Center, Iran University of Medical Sciences, Tehran, Iran

<sup>3</sup> Department of Medical Parasitology and Mycology, School of Public Health, Tehran University of Medical Sciences, Tehran, Iran

<sup>4</sup> Department of Medical Nanotechnology, School of Advanced Technologies in Medicine, Iran University of Medical Sciences, Tehran, Iran

### ARTICLE INFO

#### Article History:

Received 09 Mar 2025

Accepted 18 May 2025

Published 01 Jun 2025

#### Keywords:

Green synthesis

Gold nanoparticles

Fungicidal effect

*Aspergillus*

*Candida*

Fluconazole

Itraconazole

### ABSTRACT

**Objective(s):** The COVID-19 pandemic has underscored the global threat posed by opportunistic pathogens, including drug-resistant fungi. Metal nanoparticles are considered general microbicidal agents. These nanoparticles have a broad antimicrobial spectrum.

**Methods:** The preparation of nanoparticles with curcumin coating was performed through a single-step procedure in which curcumin acted as a reducing and stabilizing agent. The characterizations of the particles were conducted through electron microscopy, dynamic light scattering, and UV-Vis spectroscopy. The cytotoxicity of particles was evaluated with an MTT assay. The antifungal properties of curcumin-coated gold nanoparticles were evaluated up to a concentration of 128 µg/ml against different species of *Candida* and *Aspergillus*, and compared with common antifungal drugs such as fluconazole and itraconazole. TEM was applied to investigate the structural analysis of the particles' interaction.

**Results:** The particle synthesis was performed using a single-batch green method. Characterized by TEM, UV-Vis, and DLS, the particles exhibited an average diameter of  $7.5 \pm 4.1$  nm and remained stable for over 64 days. Cytotoxicity tests on HepG2 cells showed high biocompatibility. While Cur@AuNPs exhibited antifungal activity against various species of *Candida*, including drug-resistant strains, no significant activity was observed against *Aspergillus* species. These findings suggest potential applications of Cur@AuNPs in treating *Candida*-related infections.

**Conclusions:** Cur@AuNPs demonstrate inhibitory properties on different species of *Candida* but do not exhibit antifungal activity against either drug-sensitive or drug-resistant *Aspergillus* species.

### How to cite this article

Mahmoudi S., Amini SM, Khodavaissy S., Mansoori K.. Investigation of the Antifungal Activity of Curcumin-Coated Gold Nanoparticles. *Nanomed Res J*, 2025; 10(2): 179-188. DOI: 10.22034/nmrj.2025.02.009

## INTRODUCTION

Considerable evidence on the expansion of the geographical range and the incidence of dangerous fungal diseases around the world have emerged in recent years. Various reasons have been cited for the increased prevalence of dangerous fungi, including global warming, increased communication, and the

expansion of global trade (1). In recent years, the occurrence of invasive and deadly fungal infections has significantly increased among COVID-19 patients (2). Due to the widespread use of antifungal drugs for common fungal infections such as oral and vaginal *Candida* or respiratory fungi such as *Aspergillus*, the risks of more aggressive forms of infections in the general population are always

\* Corresponding Author Email: [Mohammadamini86@gmail.com](mailto:Mohammadamini86@gmail.com)

increasing. Using substances that inhibit the growth of fungi in different environments is one of the most common ways to prevent infection.

Curcumin is a natural phenol with antimicrobial characteristics against a broad spectrum of pathogens (3). This compound is hydrophobic and is not bioavailable systemically. Curcumin nanoformulations have drawn attention as a solution for this drawback because they can increase curcumin hydrophilicity and boost its bioavailability (4). Recent studies have advanced antifungal nanomaterials, demonstrating the efficacy of metal-ligand complexes in combating drug-resistant fungi through enhanced bioavailability and targeted activity (5, 6). Phytochemical-based formulations, including those inspired by curcumin, offer promising antimicrobial properties but highlight the need for eco-friendly synthesis to improve stability and reduce toxicity (7).

Apart from various medicinal properties, curcumin, as an active phytochemical compound, can be applied for the chemical synthesis of metal nanoparticles. Metal nanoparticles have widely entered in medical research (8), diagnostics (9), cancer treatments (10), health industry (11), and antimicrobial applications (12). Here the aqueous solution of Cur@AuNPs through a one pot green synthesis procedure without any other chemicals or solvent. The antifungal effect of the synthesized nanoparticles has been investigated for the first time against various strains of *Candida* and *Aspergillus* fungus.

## MATERIAL AND METHODS

### *Synthesis of the Cur@AuNPs*

Briefly, 20 mM solution of curcumin (diferuloylmethane, C<sub>21</sub>H<sub>20</sub>O<sub>6</sub>, 65%, Sigma-Aldrich, USA) in DMSO (C<sub>2</sub>H<sub>6</sub>OS, 99.5%, Gibco, Life Technologies GmbH, Karlsruhe, Germany) was prepared. A round bottom flask was filled with 15 mL of deionized water (DIW). The water's pH was adjusted to approximately 9 using a 150 mM potassium carbonate (K<sub>2</sub>CO<sub>3</sub>) solution sourced from Sigma-Aldrich, USA. Subsequently, 100 µL of curcumin solution was added dropwise into the stirred DIW, causing the initially yellow curcumin solution to shift to a red hue. After a three-minute interval, 2.5 mL of tetrachloroauric (III) acid trihydrate (HAuCl<sub>4</sub>·3H<sub>2</sub>O, 2.5 mM, Sigma-Aldrich, Germany) was slowly introduced into the curcumin mixture. The reaction was maintained

under continuous stirring for three hours, then the mixture was kept undisturbed in the dark for a period of three days. (13, 14) According to our previous study, the nanoparticles were washed through a series of centrifugation and decantation to remove unreacted reagents (15, 16).

### *Characterizations of the Cur@AuNPs*

Prior to conducting any characterization, the produced Cur@AuNPs were filtered using a 0.2 µm polyvinylidene fluoride (PVDF) membrane. Transmission electron microscopy (Zeiss EM 900, Germany) was employed to examine the size and structural features of the nanoparticles. The nanoparticles' optical characteristics were evaluated via UV-Visible spectroscopy, utilizing a double-beam UV-Vis absorption spectrophotometer (SPEKOL 2000, Analytik Jena, UK) equipped with a quartz cuvette having a 1 cm optical path length. Additionally, dynamic light scattering (DLS) measurements to determine hydrodynamic size were performed using the NANO-flex Particle Sizer (Germany), while the surface charge (zeta potential) was assessed with a Zeta-check instrument (Microtrac, Germany). Finally, the concentration of gold ions within the nanoparticle suspensions was quantified through inductively coupled plasma optical emission spectroscopy (ICP-OES).

### *In vitro cytotoxicity analysis*

HepG2 cells were obtained from the Pasteur Institute of Iran, Tehran. Cells were cultured in DMEM culture medium supplemented with 10% fetal bovine serum (FBS), and 1% penicillin-streptomycin solution. The cells were kept in an atmosphere of 5% CO<sub>2</sub> air at 37°C and the culture medium was changed daily. To investigate the cytotoxicity of Cur@AuNPs, cells were seeded at approximately 100,000 cells per well of a 96-well plate, and after the cells were attached to the plate, the cells were treated with culture containing different concentrations of nanoparticles and incubated for 24 hours. Then the cells were washed with PBS and incubated with 100 µL of MTT solution in buffer or culture medium at a concentration of 0.5 mg/mL for 2-4 hours. Following incubation, the MTT solution was removed and replaced with 100 µL of DMSO. After gently shaking the plate for 2 minutes, absorbance was measured at 570 nm using a microplate reader.

### Antifungal activity testing of Cur@AuNPs Fungal strains

A set of 30 clinically important fungal strains including *Candida albicans* (n=6), *Candida parapsilosis* (n=6), *Candida krusei* (n=6), *Aspergillus fumigatus* (n=6), and *Aspergillus flavus* (n=6) were investigated in the current study. These fungi have previously been identified using sequence analysis of ITS1-5.8S rDNA-ITS2 (for *Candida* species) or beta-tubulin (for *Aspergillus* species) markers.

### Broth dilution

The antifungal activity of Cur@AuNPs was determined according to the Clinical and Laboratory Standards Institute (CLSI) protocols for yeasts and filamentous fungi (17). The susceptibility of the isolates to itraconazole (Behvazan Co., Iran) and fluconazole (Amin Pharma. Co., Iran) was also determined using the same method. The tested concentrations for Cur@AuNPs, itraconazole, and fluconazole were 1–512 µg/mL, 0.03–16 µg/mL, and 0.125–64 µg/mL, respectively. *C. parapsilosis* ATCC 22019 and *C. krusei* ATCC 5268 were used as quality control. The value of minimum inhibitory concentration (MIC) was considered as the lowest concentration of the nanoparticle that was able to make 50% inhibition (100% for itraconazole against *Aspergillus* species) in comparison to drug-free growth control wells. Minimum fungicidal concentration (MFC) was determined based on a method described previously (18).

### Specimen preparation for electron microscopy

For analysis of the Cur@AuNPs interaction with *C. albicans*, cultures were incubated with Cur@AuNPs at 32 µg/mL concentration for 24 hours. After nanoparticle incubation, the treated microorganisms were washed with PBS carefully. For primary fixation a 2-hour incubation with 2.5% glutaraldehyde was applied. Free glutaraldehyde was removed through a series of washing procedures with PBS. Secondary fixation was carried out by 1.5-hour incubation with 1% osmium tetroxide. Dehydration of the fungus was performed in acetone (50, 70, 90, 100%), then infiltrated by resin and finally embedded in pure resin (Epon 812, TAAB, UK). then, the ultra-microtome was applied to obtain thin sections of 50 nm. Finally, the provided slices were stained with uranyl acetate and lead citrate for investigation under TEM (Zeiss EM 900, Germany)

### Software and statistics

The data are expressed as means  $\pm$  SD. Differences between groups were assessed by one-way ANOVA. The diagram was analyzed and presented using Origin 6 software. The size distribution of the particles was obtained from the Gaussian fit of the diameter of 100 nanoparticles that have been analyzed with Digital Micrograph software..

## RESULTS AND DISCUSSION

### Synthesis and characterizations

This green approach, leveraging curcumin's dual role as reductant and stabilizer, yielded stable, spherical NPs, contrasting with slower kinetics in microbial green syntheses that often yield polydisperse particles (19) or an immunogenic response similar to previous experiences for gene delivery applications (20).

The formation of Cur@AuNPs was verified by the distinct plasmonic red color typical of gold nanoparticles (21). The observation that the plasmonic peak remains at essentially the same wavelength (524 nm vs. 525 nm) over a period of more than two months is a strong and direct indicator of high stability for the Cur@AuNPs. The UV-Vis spectra were applied to investigate the stability of the particles (Figure 1). Similar nanoparticles that have been synthesized by apigenin, which is a natural flavonoid, represent high stability in physiological environments (15). The very high stability of curcumin-coated silver nanoparticles was also investigated in our previous study (22). After making sure that the stable nanoparticles were synthesized, the hydrodynamic diameter of the particles was evaluated, which was  $10.88 \pm 1.16$  nm. TEM analysis revealed the size distribution and morphological characteristics of the synthesized Cur@AuNPs. Cur@AuNPs represent spherical morphology, with an average particle size of  $7.5 \pm 4.1$  nm with all of the nanoparticles were almost spherical (Figure 2).

Studies have shown that nanoparticles produced via green synthesis often exhibit significant variability in both size and morphology (19). This heterogeneity arises because the reduction of metal ions by plant-derived compounds proceeds at a relatively slow rate, resulting in nanoparticles with a broad size distribution (23). In the preparation of Cur@AuNPs, curcumin must first be dissolved in DMSO and can then be further diluted with water, particularly at elevated pH levels. Raising the pH

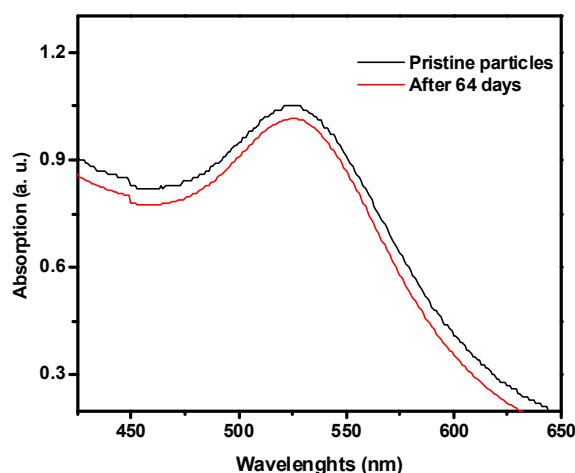


Fig. 1. The stability analysis of Cur@AuNPs over two months with UV-Vis spectroscopy.

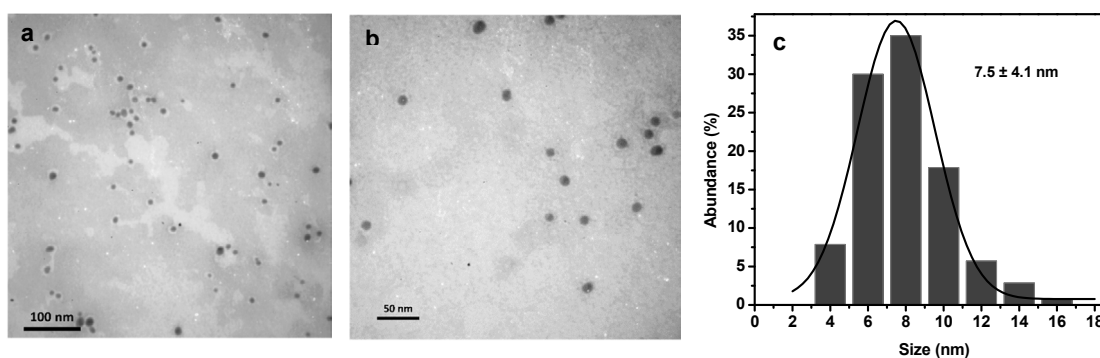


Fig. 2. Transmission electron micrographs of Cur@AuNPs (a, b) and the corresponding size distribution (c).

is crucial to facilitate the release of protons from curcumin's hydroxyl groups, which aids in the reduction of gold ions. It is important to introduce  $\text{HAuCl}_4$  within 5 minutes, as at pH 9, curcumin degradation intensifies beyond this time frame. By adding  $\text{HAuCl}_4$ , primary gold nuclei are formed with electrons obtained from the degradation of curcumin. It has been demonstrated that small silver particles can have catalytic properties in the destruction of curcumin (24). The catalytic activity of gold was also declared (14). This can provide more electrons for the reduction of gold ions in the growth stage of the nuclei. The slower the growth of the particles, the more homogeneous the shape and size of the nanoparticles will be. That is why the growth of nanoparticles at room temperature without stirring for three days was chosen. To eliminate unbound curcumin, the Cur@AuNPs underwent multiple cycles of centrifugation followed by decantation. Studies have shown

that performing this washing process four times effectively clears residual curcumin and gold ions (13, 14). The final nanoparticles had a negative charge of  $-27.9 \pm 0.1$  mV, which is actually due to the presence of the polyphenol coating caused by the polymerization of the broken curcuminoids on the surface of the nanoparticles.

#### Cytotoxicity evaluation

A key challenge in utilizing metal nanoparticles for biomedical applications is their potential toxicity. Since gold is non-biodegradable, its long-term toxicity is a concern, with cytotoxicity depending on parameters such as size, shape, and surface chemistry. For instance, studies show that traditionally synthesized citrate-coated gold nanoparticles with the size of 5 nm are more toxic than 15 or 25 nm ones (25). The use of natural phytochemicals like curcumin for synthesis has produced nanoparticles with reduced toxicity.

Curcumin-coated gold nanoparticles (Cur@AuNPs) have demonstrated high biocompatibility, showing no significant toxicity on human colorectal cancer HT29 (up to 50 µg/mL) (14), human monocytic cell line (THP-1) (26), human prostate cancer cell line (PC-3) VI paper (up to 280 µg/mL) (27), embryonic BD1X rat heart tissue (H9c2) (28), and peripheral blood mononuclear cells (PBMCs) (29). However, cytotoxic effects have been observed in other lines, such as L929 mouse fibroblastic cells (50% cell death at 120 µg/mL) (30), 3T3 Fibroblasts (31), human lung cancer (A549), human breast cancer (MDAMB-231), prostate cancer (DU145) cell lines (32), and MCF-7, as well as HCT-116 (33). In the present study on HepG2 cells, statistically significant effects begin at 4 µg/mL, yet over 90% of cells survive at 16 µg/mL (92.23%), and over 70% survive at 128 µg/mL (75.41%). By reviewing all these reports, it can be concluded that if Cur@AuNPs are washed well to remove ions, free curcumin, and other by-products not attached to the surface, the resulting nanoparticles are very biocompatible toward various cell lines.

*Antifungal activity of Cur@AuNPs*

MIC values of Cur@AuNPs, fluconazole, and itraconazole against *Aspergillus* and *Candida* isolates used in this study are shown in Table 1. All the *Aspergillus* isolates were unresponsive to fluconazole (geometric mean [GM] MIC: >64 µg/mL), while 5 and 4 isolates were susceptible and intermediate to itraconazole, respectively. Cur@AuNPs, similar to fluconazole, did not show any activity against the *Aspergillus* isolates (GM MIC: >128 µg/mL).

The lack of activity against *Aspergillus*'s species may be attributed to several structural and mechanistic factors. Differences in fungal cell wall composition could play a key role, as *Candida* species are primarily composed of β-glucans and mannans, facilitating easier nanoparticle interaction, whereas *Aspergillus* features a higher chitin content and a more rigid structure that may impede Cur@AuNP penetration or adhesion (34). Additionally, variations in curcumin release kinetics or nanoparticle uptake might differ between the genera, with *Aspergillus* filamentous morphology

Table 1. The minimum inhibitory concentration (MIC) values of curcumin-coated gold nanoparticles (Cur@AuNPs) and two comparator antifungal drugs against *Aspergillus* and *Candida* species

| No. | Species                      | Minimum Inhibitory Concentration (MIC) Values (µg/mL) and interpretations |                |              |                |           |
|-----|------------------------------|---|----------------|--------------|----------------|-----------|
|     |                              | Fluconazole   | Interpretation | Itraconazole | Interpretation | Cur@AuNPs |
| 1   | <i>Aspergillus fumigatus</i> | >64   | Resistant      | 16           | Resistant      | >128      |
| 2   | <i>Aspergillus fumigatus</i> | >64   | Resistant      | 8            | Resistant      | >128      |
| 3   | <i>Aspergillus fumigatus</i> | >64   | Resistant      | 16           | Resistant      | >128      |
| 4   | <i>Aspergillus fumigatus</i> | >64   | Resistant      | 2            | Intermediate   | >128      |
| 5   | <i>Aspergillus fumigatus</i> | >64   | Resistant      | 0.5          | Susceptible    | >128      |
| 6   | <i>Aspergillus fumigatus</i> | >64   | Resistant      | 2            | Intermediate   | >128      |
| 7   | <i>Aspergillus flavus</i>    | >64   | Resistant      | 0.5          | Susceptible    | >128      |
| 8   | <i>Aspergillus flavus</i>    | >64   | Resistant      | 1            | Susceptible    | >128      |
| 9   | <i>Aspergillus flavus</i>    | >64   | Resistant      | 0.5          | Susceptible    | >128      |
| 10  | <i>Aspergillus flavus</i>    | >64   | Resistant      | 2            | Intermediate   | >128      |
| 11  | <i>Aspergillus flavus</i>    | >64   | Resistant      | 2            | Intermediate   | >128      |
| 12  | <i>Aspergillus flavus</i>    | >64   | Resistant      | 1            | Susceptible    | >128      |
| 13  | <i>Candida albicans</i>      | >64   | Resistant      | >16          | Resistant      | 64        |
| 14  | <i>Candida albicans</i>      | >64   | Resistant      | >16          | Resistant      | 64        |
| 15  | <i>Candida albicans</i>      | >64   | Resistant      | 0.5          | Resistant      | 16        |
| 16  | <i>Candida albicans</i>      | >64   | Resistant      | >16          | Resistant      | 8         |
| 17  | <i>Candida albicans</i>      | 64  | Resistant      | 0.06         | Susceptible    | 32        |
| 18  | <i>Candida albicans</i>      | 0.25  | Susceptible    | 0.06         | Susceptible    | 16        |
| 19  | <i>Candida parapsilosis</i>  | 16  | Resistant      | 0.125        | Susceptible    | 32        |
| 20  | <i>Candida parapsilosis</i>  | 16  | Resistant      | 0.125        | Susceptible    | 16        |
| 21  | <i>Candida parapsilosis</i>  | 16  | Resistant      | 0.25         | Resistant      | 64        |
| 22  | <i>Candida parapsilosis</i>  | 16  | Resistant      | 0.06         | Susceptible    | 128       |
| 23  | <i>Candida parapsilosis</i>  | 0.5   | Susceptible    | 0.06         | Susceptible    | 64        |
| 24  | <i>Candida parapsilosis</i>  | 2   | Resistant      | 0.25         | Resistant      | 64        |
| 25  | <i>Candida krusei</i>        | >64   | Resistant      | 0.25         | Not applicable | 64        |
| 26  | <i>Candida krusei</i>        | 64  | Resistant      | 0.25         | Not applicable | 32        |
| 27  | <i>Candida krusei</i>        | 64  | Resistant      | 16           | Not applicable | 32        |
| 28  | <i>Candida krusei</i>        | 64  | Resistant      | 0.25         | Not applicable | 64        |
| 29  | <i>Candida krusei</i>        | 64  | Resistant      | 0.25         | Not applicable | 128       |
| 30  | <i>Candida krusei</i>        | >64   | Resistant      | 0.25         | Not applicable | 32        |



potentially leading to reduced internalization compared to the yeast-like form of *Candida* (22). Furthermore, fungal efflux pumps and inherent drug resistance mechanisms in *Aspergillus*, such as those contributing to azole tolerance, could actively expel curcumin or limit Cur@AuNP efficacy (35). These observations align with studies on curcumin nanoformulations, which often show stronger antifungal effects against *Candida* than *Aspergillus* due to these biological barriers (4). Future experiments, including comparative uptake assays using fluorescently labeled nanoparticles, efflux pump inhibitor co-treatments, or cell wall disruption models, could further elucidate these mechanisms and guide optimizations for broader-spectrum activity.

The fungistatic effect of citrate-capped gold nanoparticles (36), and NaBH<sub>4</sub>-capped gold nanoparticles (37) was declared for *Candida* strains. Since the nanoparticles made with these chemicals do not have steric stability, they are very unstable in physiological environments. Therefore, they cannot be easily used for biomedical applications. These chemicals themselves have toxic effects on eukaryotic cells and their removal from the surface or solution of nanoparticles cannot be done easily (37). Even the comparative study of nanoparticles has shown that nanoparticles prepared with NaBH<sub>4</sub> have more toxicity than the same nanoparticles that have been prepared by SnCl<sub>2</sub> against *Candida* strains (37).

Regarding the *Candida* species, all but two (one *C. albicans* [MIC: 0.25 µg/mL] and one *C. parapsilosis* [MIC: 0.5 µg/mL] isolates), were resistant to fluconazole. There were also four isolates with MIC values of ≥16 µg/mL for itraconazole. The activity of Cur@AuNPs was much better against *Candida* species, with the superiority of *C. albicans*, compared to *Aspergillus* species. The GM MICs of Cur@AuNPs against *C. albicans*, *C. parapsilosis*, and *C. krusei* isolates were 25.40 µg/mL, 50.80 µg/mL, and 50.80 µg/mL, respectively. The inhibition activity of the curcumin against the *Candida* strains was attributed to hyphal development suppression by Cur (38). Also, the production of reactive oxygen species (ROS) from Cur (39), and gold nanoparticles has been reported (40). Regarding the MFC values, Cur@AuNPs did not demonstrate any fungicidal activity against *Aspergillus* and *Candida* species. The activity of itraconazole in this regard was much better than the fluconazole and Cur@AuNPs (Table 2).

Antifungal effects of gold nanoparticles with similar biogenic coatings on *Aspergillus* strains have been investigated in some studies. Such coatings for gold nanoparticles prepared by green chemistry method can be from all compounds of an extract of a substance such as a plant or mushroom, or a phytochemical isolated from an extract. Antifungal effects against the *Aspergillus flavus* strain have been observed for gold nanoparticles prepared with *Agaricus bisporus* mushroom extract. However, other strains of *Aspergillus* were resistant to the synthesized nanoparticles (41).

Antifungal effect toward *Aspergillus flavus*, *Aspergillus niger*, and *Candida albicans* for green synthesized gold nanoparticles from *Abelmoschus esculentus* extract was also demonstrated (42). Green-synthesized gold nanoparticles from *Cannabis sativa* represent an inhibitory effect against *Aspergillus flavus*, *Aspergillus fumigatus*, and *Aspergillus niger* (43). Quercetin is a natural flavonoid that could be applied for the synthesis of gold nanoparticles. The inhibitory effect of quercetin against *A. fumigatus* was reported by Milanezi et al (44). Cinnamaldehyde is the main flavonoid from the spice cinnamon and has been applied for the synthesis of gold nanoparticles. The synthesized Cinnamaldehyde-coated gold nanoparticles could inhibit the *C. albicans* at the 75 µg/ml concentration (45).

To evaluate the interaction between nanoparticles and fungal species, transmission electron microscopy imaging of the fungi treated with Cur@AuNPs was performed (Figure 4). The interaction of Cur@AuNPs with the *Candida albicans* samples could be classified into three categories based on the provided micrographs. It was observed that the Cur@AuNPs are accumulated on the surface of the cell wall/membrane (black arrows). This accumulation of nanoparticles on the cell wall can also have a negative effect on the process of cell mitosis. An example of a dividing cell is marked by a white line in the micrograph of Figure 4a. The interaction of metal nanoparticles on microorganisms' membranes could also disturb the membrane potential and create pores. This phenomenon leads to disruption of the microorganism's cell membrane/wall and the exit of ions and cytoplasmic fluid from the microorganism. The cell wall disruptor (orange arrows), and cytoplasmic shedding (green arrows) are observed in the presented TEM micrographs. The entrance of the Cur@AuNPs into the cytoplasm

Table 2. The minimum fungicidal concentration (MFC) values of curcumin-coated gold nanoparticles (Cur@AuNPs) and two comparator antifungal drugs against *Aspergillus* and *Candida* species

| No. | Species                      | Minimum fungicidal concentration (MFC) values vales (µg/mL) |              |           |
|-----|------------------------------|---|--------------|-----------|
|     |                              | Fluconazole   | Itraconazole | Cur@AuNPs |
| 1   | <i>Aspergillus fumigatus</i> | >64   | >16          | >128      |
| 2   | <i>Aspergillus fumigatus</i> | >64   | >16          | >128      |
| 3   | <i>Aspergillus fumigatus</i> | >64   | >16          | >128      |
| 4   | <i>Aspergillus fumigatus</i> | >64   | 8            | >128      |
| 5   | <i>Aspergillus fumigatus</i> | >64   | 4            | >128      |
| 6   | <i>Aspergillus fumigatus</i> | >64   | 8            | >128      |
| 7   | <i>Aspergillus flavus</i>    | >64   | 2            | >128      |
| 8   | <i>Aspergillus flavus</i>    | >64   | 4            | >128      |
| 9   | <i>Aspergillus flavus</i>    | >64   | 4            | >128      |
| 10  | <i>Aspergillus flavus</i>    | >64   | 8            | >128      |
| 11  | <i>Aspergillus flavus</i>    | >64   | 16           | >128      |
| 12  | <i>Aspergillus flavus</i>    | >64   | 4            | >128      |
| 13  | <i>Candida albicans</i>      | >64   | >16          | >128      |
| 14  | <i>Candida albicans</i>      | >64   | >16          | >128      |
| 15  | <i>Candida albicans</i>      | >64   | 8            | >128      |
| 16  | <i>Candida albicans</i>      | >64   | >16          | >128      |
| 17  | <i>Candida albicans</i>      | >64   | 2            | >128      |
| 18  | <i>Candida albicans</i>      | 1   | 1            | >128      |
| 19  | <i>Candida parapsilosis</i>  | >64   | 4            | >128      |
| 20  | <i>Candida parapsilosis</i>  | >64   | 4            | >128      |
| 21  | <i>Candida parapsilosis</i>  | >64   | 4            | >128      |
| 22  | <i>Candida parapsilosis</i>  | >64   | 2            | >128      |
| 23  | <i>Candida parapsilosis</i>  | >64   | 1            | >128      |
| 24  | <i>Candida parapsilosis</i>  | 2   | 2            | >128      |
| 25  | <i>Candida krusei</i>        | >64   | 4            | >128      |
| 26  | <i>Candida krusei</i>        | >64   | 2            | >128      |
| 27  | <i>Candida krusei</i>        | >64   | >16          | >128      |
| 28  | <i>Candida krusei</i>        | >64   | 4            | >128      |
| 29  | <i>Candida krusei</i>        | >64   | 4            | >128      |
| 30  | <i>Candida krusei</i>        | >64   | 2            | >128      |

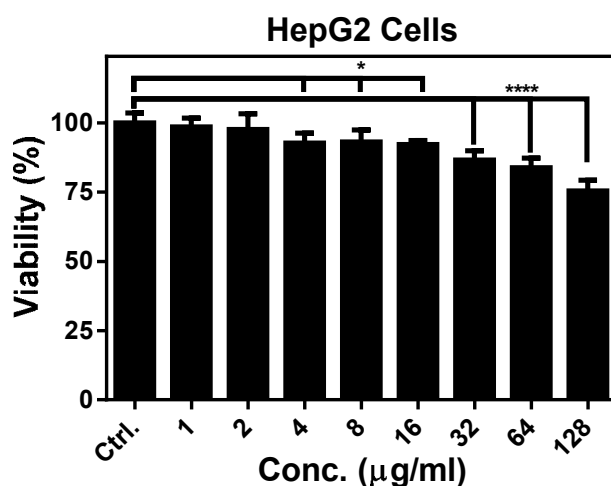


Fig. 3. Cytotoxicity evaluation of Cur@AuNPs on HepG2 cells. 24-hour treatment was applied. (Asterisks point out statistically significant differences: \*P < 0.05 and \*\*\*\*P < 0.0001).

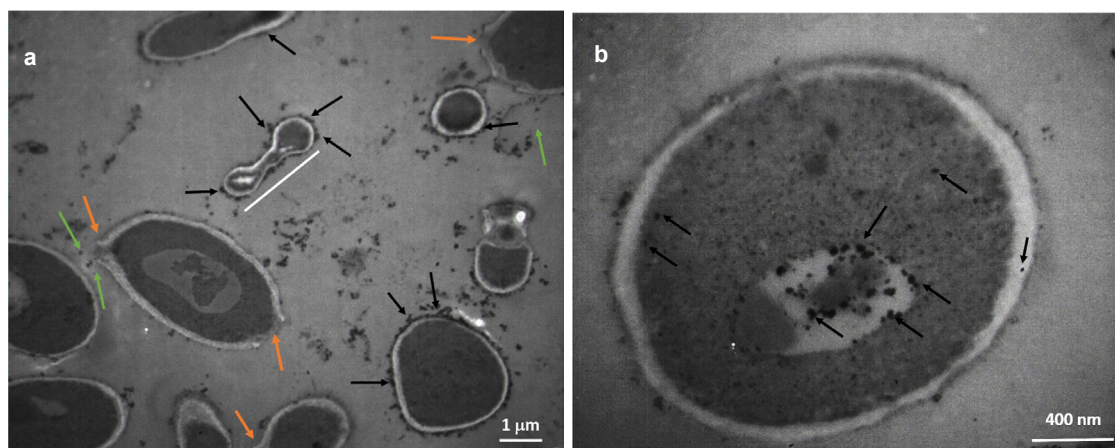


Fig. 4. Transmission electron micrographs of *Candida albicans* that have been treated with Cur@AuNPs at the concentration of 32 mg/ml. TEM images revealed Cur@AuNPs localized on the fungal cell wall (black arrows) (a), with additional particles observed disrupting the membrane and entering the cytoplasm and organelles (b). Orange arrows indicate the cell membrane/wall disruptor (a) and the green arrows indicate the shedding of cytoplasm from the rupture site (a).

of the intact fungal cell is also clear in the TEM micrographs (Figure 4b-c).

## CONCLUSION

The synthesis of biocompatible gold nanoparticles with the natural phenolic compound curcumin was performed through a single-step method in which curcumin acts both as a metal ion-reducing agent and as a stabilizing and coating agent. The synthesized Cur@AuNPs demonstrated high biocompatibility, with over 90% HepG2 cell viability observed at concentrations up to 16 µg/mL. Cur@AuNPs exhibited promising antifungal activity against various *Candida* species, including drug-resistant strains, but were ineffective against *Aspergillus* species. These results highlight the potential of Cur@AuNPs as alternative agents for *Candida*-related infections.

## ACKNOWLEDGMENTS

This study has been funded by Iran University of Medical Sciences (IUMS) under grant number 1402-3-68-26809.

## DECLARATION OF INTEREST

None.

## ETHICS DECLARATION

This is an *in vitro* study. The Iran University of Medical Sciences Research Ethics Committee has approved under IR.IUMS.REC.1399.913 code.

## REFERENCES

1. Antimicrobial Resistance AR. WHO releases first-ever list of health-threatening fungi. World Health Organization; 2022.
2. Hoenigl M, Seidel D, Sprute R, Cunha C, Oliverio M, Goldman GH, et al. COVID-19-associated fungal infections. *Nat Microbiol.* 2022;7(8):1127-40. <https://doi.org/10.1038/s41564-022-01172-2>
3. Alsammarraie FK, Wang W, Zhou P, Mustapha A, Lin M. Green synthesis of silver nanoparticles using turmeric extracts and investigation of their antibacterial activities. *Colloids Surf B Biointerfaces.* 2018;171:398-405. <https://doi.org/10.1016/j.colsurfb.2018.07.059>
4. Trigo-Gutierrez JK, Vega-Chacón Y, Soares AB, Mima EGdO. Antimicrobial activity of curcumin in nanoformulations: a comprehensive review. *Int J Mol Sci.* 2021;22(13):7130. <https://doi.org/10.3390/ijms22137130>
5. Tahiri NEH, Soulo N, El Ghouzi A, Saghrouchni H, El Khomsi M, Ousaad D, et al. Volatile profile, in silico toxicity prediction, and antioxidant and antimicrobial activities of *Laurus nobilis* L. essential oil from distinct geographical locations. *Chem Rev Lett.* 2024;7(5):884-94.
6. Malekhoseini A, Montazerzohori M, Naghihi R, Panahi Kokhdan E, Joohari S. Antimicrobial/antioxidant and cytotoxicity activities of some new mercury(II) complexes. *Chem Rev Lett.* 2023;6(2):166-82.
7. Emenike EC, Onyema C. Phytochemical, Heavy Metals and Antimicrobial Study of the Leaves of *Calopogonium mucunoides*. *J Chem Lett.* 2022;3(1):30-7. <https://doi.org/10.21203/rs.3.rs-1097372/v1>
8. Mahabadi VP, Amini SM, Jameie SB, Farhadi M, Eslahi N. A study of sleep-wake cycle after transplantation of neural stem cells treated with gold nanoparticles in the suprachiasmatic nucleus lesion in the rat. *Nanomed Res J.* 2025;9(3):308-16.
9. Amini SM, Baniasadipour B, Bagheri F, Berenji M. Recent advances in magnetic resonance imaging using metal-or-

- ganic frameworks. *Chin J Acad Radiol*. 2025;Forthcoming. <https://doi.org/10.1007/s42058-025-00195-y>
10. Sharifkazemi H, Amini SM, Ortakand RK, Narouie B. A Review of Photodynamic Therapy in Different Types of Tumors. *Transl Res Urol*. 2022;4(2):61-70.
  11. Amini SM, Mahabadi VP. Selenium nanoparticles role in organ systems functionality and disorder. *Nanomed Res J*. 2018;3(3):117-24.
  12. Shahmoradi S, Shariati A, Amini SM, Zargar N, Yadegari Z, Darban-Sarokhalil D. The application of selenium nanoparticles for enhancing the efficacy of photodynamic inactivation of planktonic communities and the biofilm of *Streptococcus mutans*. *BMC Res Notes*. 2022;15(1):290. <https://doi.org/10.1186/s13104-022-05973-w>
  13. Amini SM, Shahroodian S. Antibacterial activity of silver and gold nanoparticles that have been synthesized by curcumin. *Inorg Nano-Met Chem*. 2023;53(1):1-7.
  14. Akbari A, Shokati Eshkiki Z, Mayahi S, Amini SM. In-vitro investigation of curcumin coated gold nanoparticles effect on human colorectal adenocarcinoma cell line. *Nanomed Res J*. 2022;7(1):66-72.
  15. Mohammadi E, Amini SM. Green synthesis of stable and biocompatible silver nanoparticles with natural flavonoid apigenin. *Nano-Struct Nano-Objects*. 2024;38:101175. <https://doi.org/10.1016/j.nanoso.2024.101175>
  16. Amini SM, Kakolvand R, Taeb S, Valizadeh H. Investigating the synthesis of tellurium nanoparticles and investigating its physicochemical and toxicological properties on fibroblast cells. *Nanomed Res J*. 2024;9(4):373-80.
  17. Clinical and Laboratory Standards Institute. Reference Method for Broth Dilution Antifungal Susceptibility Testing of Yeasts; Approved Standard-Third Edition. CLSI document M27-A3. Wayne, PA: CLSI; 2017.
  18. Mahmoudi S, Zaini F, Kordbacheh P, Safara M, Heidari M. *Sporothrix schenckii* complex in Iran: molecular identification and antifungal susceptibility. *Sabouraudia*. 2016;54(6):593-9. <https://doi.org/10.1093/mmy/myw006>
  19. Salavati MS, Amini SM, Nooshadokht M, Shahabi A, Sharifi F, Afsar A, et al. Enhanced Colloidal Stability of Silver Nanoparticles by Green Synthesis Approach: Characterization and Anti-Leishmaniasis Activity. *Nano*. 2022;17(07):2250052. <https://doi.org/10.1142/S1793292022500527>
  20. Thomas CE, Ehrhardt A, Kay MA. Progress and problems with the use of viral vectors for gene therapy. *Nat Rev Genet*. 2003;4(5):346-58. <https://doi.org/10.1038/nrg1066>
  21. Esmaeili-bandboni A, Amini SM, Faridi-Majidi R, Bagheri J, Mohammadnejad J, Sadroddiny E. Cross-linking gold nanoparticles aggregation method based on localised surface plasmon resonance for quantitative detection of miR-155. *IET Nanobiotechnol*. 2018;12(4):453-8. <https://doi.org/10.1049/iet-nbt.2017.0174>
  22. Amini SM, Getso MI, Farahyar S, Khodavaisy S, Roudbary M, Mahabadi VP, et al. Antifungal activity of green-synthesized curcumin-coated silver nanoparticles alone and in combination with fluconazole and itraconazole against *Candida* and *Aspergillus* species. *Curr Med Mycol*. 2023;9(3):38-44.
  23. Neshastehriz A, Hormozi-Moghadda Z, Amini S, Taheri S, Kichi ZA. Combined sonodynamic therapy and X-ray radiation with methylene blue and gold nanoparticles coated with apigenin: Impact on MCF7 cell viability. *Int J Radiat Res*. 2024;22(2):509-13. <https://doi.org/10.61186/ijrr.22.2.515>
  24. Cañameres MV, Garcia-Ramos JV, Sanchez-Cortes S. Degradation of curcumin dye in aqueous solution and on Ag nanoparticles studied by ultraviolet-visible absorption and surface-enhanced Raman spectroscopy. *Appl Spectrosc*. 2006;60(12):1386-91. <https://doi.org/10.1366/000370206779321337>
  25. Amini SM, Kharrazi S, Hadizadeh M, Fateh M, Saber R. Effect of gold nanoparticles on photodynamic efficiency of 5-aminolevulinic acid photosensitizer in epidermal carcinoma cell line: an in vitro study. *IET Nanobiotechnol*. 2013;7(4):151-6. <https://doi.org/10.1049/iet-nbt.2013.0021>
  26. Henrique TB, Alencar CA, Luis BW, Coronato CL. Synthesis and Characterization of Curcumin Gold Nanoparticles: Sonosensitizer Agent for Atherosclerosis. *J Nanosci Nanotechnol*. 2023;23(5):1-8.
  27. Nambiar S, Osei E, Fleck A, Darko J, Mutsaers AJ, Wettig S. Synthesis of curcumin-functionalized gold nanoparticles and cytotoxicity studies in human prostate cancer cell line. *Appl Nanosci*. 2018;8(3):347-57. <https://doi.org/10.1007/s13204-018-0728-6>
  28. Sharifiaghdam Z, Dalouchi F, Sharifiaghdam M, Shaabani E, Ramezani F, Nikbakht F, et al. Curcumin-coated gold nanoparticles attenuate doxorubicin-induced cardiotoxicity via regulating apoptosis in a mouse model. *Clin Exp Pharmacol Physiol*. 2022;49(1):70-83. <https://doi.org/10.1111/1440-1681.13579>
  29. Sindhu K, Rajaram A, Sreeram K, Rajaram R. Curcumin conjugated gold nanoparticle synthesis and its biocompatibility. *RSC Adv*. 2014;4(4):1808-18. <https://doi.org/10.1039/C3RA45345F>
  30. Shaabani E, Amini SM, Kharrazi S, Tajerian R. Curcumin coated gold nanoparticles: synthesis, characterization, cytotoxicity, antioxidant activity and its comparison with citrate coated gold nanoparticles. *Nanomed J*. 2017;4(2):115-25.
  31. Adlia A, Tomagola I, Damayanti S, Mulya A, Rachmawati H. Antifibrotic activity and in Ovo toxicity study of liver-targeted curcumin-gold nanoparticle. *Sci Pharm*. 2018;86(4):41. <https://doi.org/10.3390/scipharm86040041>
  32. Sreelakshmi C, Goel N, Datta K, Adlagatta A, Ummanni R, Reddy B. Green synthesis of curcumin capped gold nanoparticles and evaluation of their cytotoxicity. *Nanosci Nanotechnol Lett*. 2013;5(12):1258-65. <https://doi.org/10.1166/nml.2013.1678>
  33. Elbially NS, Abdelfatah EA, Khalil WA. Antitumor activity of curcumin-green synthesized gold nanoparticles: In vitro study. *BioNanoScience*. 2019;9(4):813-20. <https://doi.org/10.1007/s12668-019-00660-w>
  34. Latgé J-P, Beauvais A, Chamilos G. The cell wall of the human fungal pathogen *Aspergillus fumigatus*: biosynthesis, organization, immune response, and virulence. *Annu Rev Microbiol*. 2017;71(1):99-116. <https://doi.org/10.1146/annurev-micro-030117-020406>
  35. Pérez-Cantero A, López-Fernández L, Guarro J, Capilla J. Azole resistance mechanisms in *Aspergillus*: update and recent advances. *Int J Antimicrob Agents*. 2020;55(1):105807. <https://doi.org/10.1016/j.ijantimicag.2019.09.011>
  36. Rahimi H, Roudbarmohammadi S, Delavari HH, Roudbary M. Antifungal effects of indolicidin-conjugated gold nanoparticles against fluconazole-resistant strains of *Candida albicans* isolated from patients with burn infection. *Int J Nanomedicine*. 2019;14:5323-38. <https://doi.org/10.2147/IJN.S207527>
  37. Ahmad T, Wani IA, Lone IH, Ganguly A, Manzoor N,

- Ahmad A, et al. Antifungal activity of gold nanoparticles prepared by solvothermal method. *Mater Res Bull.* 2013;48(1):12-20. <https://doi.org/10.1016/j.materresbull.2012.09.069>
38. Shahzad M, Sherry L, Rajendran R, Edwards CA, Combet E, Ramage G. Utilising polyphenols for the clinical management of *Candida albicans* biofilms. *Int J Antimicrob Agents.* 2014;44(3):269-73. <https://doi.org/10.1016/j.ijantimicag.2014.05.017>
39. Alalwan H, Rajendran R, Lappin DF, Combet E, Shahzad M, Robertson D, et al. The anti-adhesive effect of curcumin on *Candida albicans* biofilms on denture materials. *Front Microbiol.* 2017;8:659. <https://doi.org/10.3389/fmicb.2017.00659>
40. Seong M, Lee DG. Reactive oxygen species-independent apoptotic pathway by gold nanoparticles in *Candida albicans*. *Microbiol Res.* 2018;207:33-40. <https://doi.org/10.1016/j.micres.2017.11.003>
41. Eskandari-Nojedehe M, Jafarizadeh-Malmiri H, Rahbar-Shahrouzi J. Hydrothermal green synthesis of gold nanoparticles using mushroom (*Agaricus bisporus*) extract: physico-chemical characteristics and antifungal activity studies. *Green Process Synth.* 2018;7(1):38-47. <https://doi.org/10.1515/gps-2017-0004>
42. Jayaseelan C, Ramkumar R, Rahuman AA, Perumal P. Green synthesis of gold nanoparticles using seed aqueous extract of *Abelmoschus esculentus* and its antifungal activity. *Ind Crops Prod.* 2013;45:423-9. <https://doi.org/10.1016/j.indcrop.2012.12.019>
43. Hameed S, Ali Shah S, Iqbal J, Numan M, Muhammad W, Junaid M, et al. Cannabis sativa-mediated synthesis of gold nanoparticles and their biomedical properties. *Bioinspired Biomim Nanobiomaterials.* 2019;9(2):95-102. <https://doi.org/10.1680/jbibr.19.00023>
44. Milanezi FG, Meireles LM, de Christo Scherer MM, de Oliveira JP, da Silva AR, de Araujo ML, et al. Antioxidant, antimicrobial and cytotoxic activities of gold nanoparticles capped with quercetin. *Saudi Pharm J.* 2019;27(7):968-74. <https://doi.org/10.1016/j.jsps.2019.07.005>
45. Ramasamy M, Lee J-H, Lee J. Direct one-pot synthesis of cinnamaldehyde immobilized on gold nanoparticles and their antibiofilm properties. *Colloids Surf B Biointerfaces.* 2017;160:639-48. <https://doi.org/10.1016/j.colsurfb.2017.10.018>